

Impact of nuclear dependence of $R = \sigma_L/\sigma_T$ on antishadowing in nuclear structure functionsVadim Guzey,¹ Lingyan Zhu,¹ Cynthia E. Keppel,¹ M. Eric Christy,¹ Dave Gaskell,² Patricia Solvignon,² and Alberto Accardi^{1,2}¹Hampton University, Hampton, Virginia 23668, USA²Thomas Jefferson National Accelerator Facility, Newport News, Virginia 23606, USA

(Received 12 July 2012; published 4 October 2012)

We study the impact of the nuclear dependence of $R = \sigma_L/\sigma_T$ on the extraction of the F_2^A/F_2^D and F_1^A/F_1^D structure function ratios from the data on the σ^A/σ^D cross section ratios. Guided by indications of the nuclear dependence of R from the world data, we examine selected sets of the European Muon Collaboration (EMC), Bologna-CERN-Dubna-Munich-Saclay (BCDMS), the New Muon Collaboration (NMC), and SLAC data and find that $F_1^A/F_1^D < \sigma^A/\sigma^D \leq F_2^A/F_2^D$. In particular, we observe that the nuclear enhancement (antishadowing) for F_1^A/F_1^D in the interval $0.1 < x < 0.3$ becomes significantly reduced or even disappears, which indicates that antishadowing is dominated by the longitudinal structure function F_L . We also argue that precise measurements of nuclear modifications of R and F_L^A have the potential to constrain the poorly known gluon distribution in nuclei over a wide range of x .

DOI: [10.1103/PhysRevC.86.045201](https://doi.org/10.1103/PhysRevC.86.045201)

PACS number(s): 13.60.Hb, 24.85.+p

I. INTRODUCTION

Since the early lepton scattering experiments that discovered the substructure of the nucleon and eventually led to the development of quantum chromodynamics (QCD) as the theory of the strong interaction, deep inelastic scattering (DIS) has been a critical tool in the investigation of the quark and gluon structure of nucleons and nuclei. While initially nuclear effects in DIS were thought to be largely negligible, this was proven wrong by the measurement of the ratio of the iron to deuterium structure functions performed by the European Muon Collaboration (EMC) at CERN in 1983 [1]. The apparent disagreement between the dramatic deviation of the ratio from unity seen in the EMC data and the small nuclear effects predicted by theoretical calculations has triggered a series of further measurements and theoretical investigations (for reviews, see [2–5]).

The emerging picture of nuclear modifications of the nucleus to deuteron cross section ratio, σ^A/σ^D , has the pattern presented in Fig. 1. For small values of Bjorken x , $x < 0.05$ – 0.1 , the ratio is noticeably suppressed—the suppression increases with an increase of the atomic number A and a decrease of x —which is called nuclear shadowing. For $0.1 < x < 0.3$, the ratio is enhanced; the effect is small (of the order of a few percent) and does not reveal an obvious A dependence. In the interval $0.3 < x < 0.8$, the ratio is suppressed and this suppression is called the EMC effect. Finally, for $x > 0.8$ the ratio dramatically grows above unity, which is explained by the effect of the nucleon motion inside nuclei (Fermi motion). Various models describe the experimental σ^A/σ^D cross section ratios for certain ranges of Bjorken x , but there is no comprehensive understanding of the entire pattern of the nuclear modifications described above. In particular, there is no unique and generally accepted theory to explain the nature of the antishadowing and EMC effects.

In this paper we focus on the enhancement (antishadowing) of the σ^A/σ^D cross section ratios in the $0.1 < x < 0.3$ region. The deviation of σ^A/σ^D from unity in the antishadowing region is of the order of a few percent [2–5] (see Fig. 1). Given

that most measurements quote normalization uncertainties on the order of 1%–2% (usually due to target thickness or luminosity), it is difficult to quantify the absolute size of the antishadowing effect precisely, and comparisons between experiments are somewhat complicated. In addition, systematic uncertainties due to radiative corrections are highly nontrivial in this region of x and are sometimes hard to determine accurately. An example of the difficulty involved in achieving very precise measurements in the antishadowing region can be found in the SLAC E139 results. The preliminary results for the Fe/D ratio were essentially consistent with unity for the region $0.1 < x < 0.3$ [9]. However, the final E139 analysis yielded results in the antishadowing region more consistent with, e.g., the EMC and BCDMS experiments, showing a small enhancement of $\approx 3\%$ on average [7]. Despite the difficulties inherent in antishadowing measurements, the results from various experiments are remarkably consistent within their experimental uncertainties. In addition, the small enhancement seen by the EMC, BCDMS, and SLAC E139 experiments for copper and iron targets has also been seen in lighter targets (Ca/D, N/D, C/D, and He/D) by the New Muon Collaboration (NMC) [10] and HERMES [11] experiments.

The antishadowing effect has rather intriguing features. Unlike the shadowing effect, antishadowing showed little or no sensitivity to the mass number A within experimental uncertainties, for example, in the SLAC E139 [7] and NMC data [10]. While antishadowing is observed in nuclear DIS, the cross section enhancement is not seen in nuclear Drell-Yan rates [12] or in total neutrino-nucleus cross sections for $x > 0.1$ [13].

In the leading twist formalism, the small enhancement of σ^A/σ^D in the antishadowing region translates into an enhancement of the valence quark and possibly gluon distributions in nuclei in this region [13–17]. However, the pattern and especially the magnitude of nuclear modifications of the gluon distribution in nuclei are very poorly constrained by present data.

The aim of this paper is to examine the impact of the nuclear dependence of $R = \sigma_L/\sigma_T$, i.e., the ratio of the longitudinal to transverse photoabsorption cross sections, on

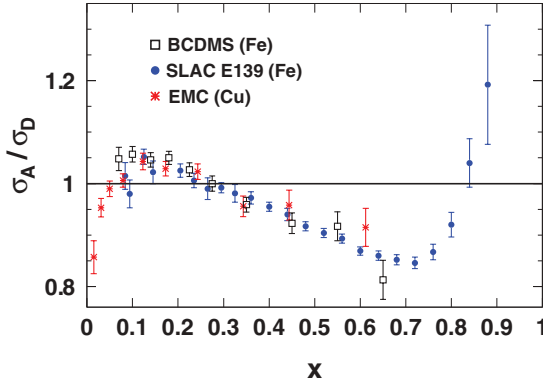


FIG. 1. (Color online) The pattern of nuclear modifications of the σ^A/σ^D cross section ratio as a function of Bjorken x for ^{56}Fe and ^{64}Cu . The data are from Bologna-CERN-Dubna-Munich-Saclay (BCDMS) [6] (open squares), SLAC E139 [7] (filled circles), and EMC [8] (stars). For all data sets statistical and systematic errors have been combined in quadrature.

the extraction of the nucleus to deuteron structure function ratios, F_2^A/F_2^D and F_1^A/F_1^D , from σ^A/σ^D data. In particular, we demonstrate that in the presence of a small but nonzero difference between R for nuclei and the nucleon, the nuclear enhancement in the ratio of the transverse structure functions F_1^A/F_1^D becomes significantly reduced (or even disappears in some cases), indicating that antishadowing is dominated by the longitudinal contribution. In addition, we analyze how the nuclear dependence of R affects the nuclear gluon distribution and emphasize the importance of measurements of R in the DIS kinematics as a direct probe of the gluon distribution in nuclei.

II. NUCLEAR DEPENDENCE OF R AND THE RATIO OF NUCLEUS AND DEUTERON STRUCTURE FUNCTIONS

A. Longitudinal contribution to the inclusive cross section

In the one-photon exchange approximation, the spin-independent cross section for inclusive electron scattering can be expressed as

$$\begin{aligned} \frac{d^2\sigma}{d\Omega dE'} &= \Gamma[\sigma_T(x, Q^2) + \epsilon\sigma_L(x, Q^2)] \\ &= \Gamma\sigma_T(x, Q^2)[1 + \epsilon R(x, Q^2)], \end{aligned} \quad (1)$$

where σ_T (σ_L) is the cross section for photoabsorption of purely transversely (longitudinally) polarized photons, $R = \sigma_L/\sigma_T$, Γ is the transverse virtual photon flux, and ϵ is the virtual photon polarization parameter. In the laboratory frame, the negative four-momentum squared (virtuality) of the exchanged photon is $-q^2 = Q^2 = 4EE'\sin^2(\theta/2)$ and the Bjorken x is $x = Q^2/[2M(E - E')]$, where E (E') is the energy of the incident (scattered) electron, θ is the scattering angle, and M is the nucleon mass. The flux of transverse virtual photons can be expressed as $\Gamma = \alpha E'(W^2 - M^2)/[4\pi^2 Q^2 M E(1 - \epsilon)]$, where α is the fine structure constant and W is the invariant energy of the virtual photon-proton system. Finally, the virtual

photon polarization parameter is

$$\begin{aligned} \epsilon &= \left[1 + 2 \left(1 + \frac{\nu^2}{Q^2} \right) \tan^2 \frac{\theta}{2} \right]^{-1} \\ &= \frac{1 - y - \frac{M^2 x^2 y^2}{Q^2}}{1 - y + \frac{y^2}{2} + \frac{M^2 x^2 y^2}{Q^2}}. \end{aligned} \quad (2)$$

where $\nu = E - E'$; $y = \nu/E$. Note that in the second line of Eq. (2) we expressed ϵ in a Lorentz-invariant form.

In terms of the structure functions $F_1(x, Q^2)$ and $F_2(x, Q^2)$ in the DIS region, the double differential cross section can be written as

$$\begin{aligned} \frac{d^2\sigma}{d\Omega dE'} &= \Gamma \frac{4\pi^2\alpha}{x(W^2 - M^2)} \\ &\times \left\{ 2xF_1 + \epsilon \left[\left(1 + \frac{4M^2x^2}{Q^2} \right) F_2 - 2xF_1 \right] \right\}. \end{aligned} \quad (3)$$

A comparison of Eqs. (1) and (3) shows that $F_1(x, Q^2)$ is purely transverse, while

$$F_L(x, Q^2) = \left(1 + \frac{4M^2x^2}{Q^2} \right) F_2(x, Q^2) - 2xF_1(x, Q^2) \quad (4)$$

is purely longitudinal. Note that $F_2(x, Q^2)$ is a mixture of both the longitudinal and transverse contributions. Thus, the ratio R is

$$R \equiv \frac{\sigma_L}{\sigma_T} = \frac{F_L(x, Q^2)}{2xF_1(x, Q^2)}. \quad (5)$$

The nucleon structure function $F_2(x, Q^2)$ is proportional to the $d^2\sigma/(d\Omega dE')$ differential cross section in the $\epsilon \rightarrow 1$ limit; it has been measured with high precision in various x and Q^2 bins. The longitudinal structure function $F_L(x, Q^2)$, in contrast, is not measured as well as $F_2(x, Q^2)$: the data are sparse and imprecise for the proton and are even more limited for nuclei. It is an experimental challenge to separate $F_2(x, Q^2)$ and $F_L(x, Q^2)$, which is usually done using the method of Rosenbluth separation, i.e., by measuring the cross section at different energies (at fixed x and Q^2) to allow for a variation of ϵ .

In this paper we shall use the parametrization of R for the nucleon, R^N , that was obtained as the result of the global analysis of the SLAC hydrogen and deuterium data [18]. The same analysis also showed that $R^D = R^H$ to high accuracy, where R^D (R^H) refers to deuterium (hydrogen). An example of the values of R^N in the kinematics used in this paper is presented in the middle panel of Fig. 2. Note that the more recent analysis of the SLAC E143 Collaboration [19] reported results for R^N consistent with those of Ref. [18].

B. Hints of nontrivial nuclear dependence of R

Experimentally measured cross section ratios contain both transverse and longitudinal contributions of the structure functions. In terms of the structure function $F_2(x, Q^2)$, one can write the ratio of the nucleus to deuteron photoabsorption

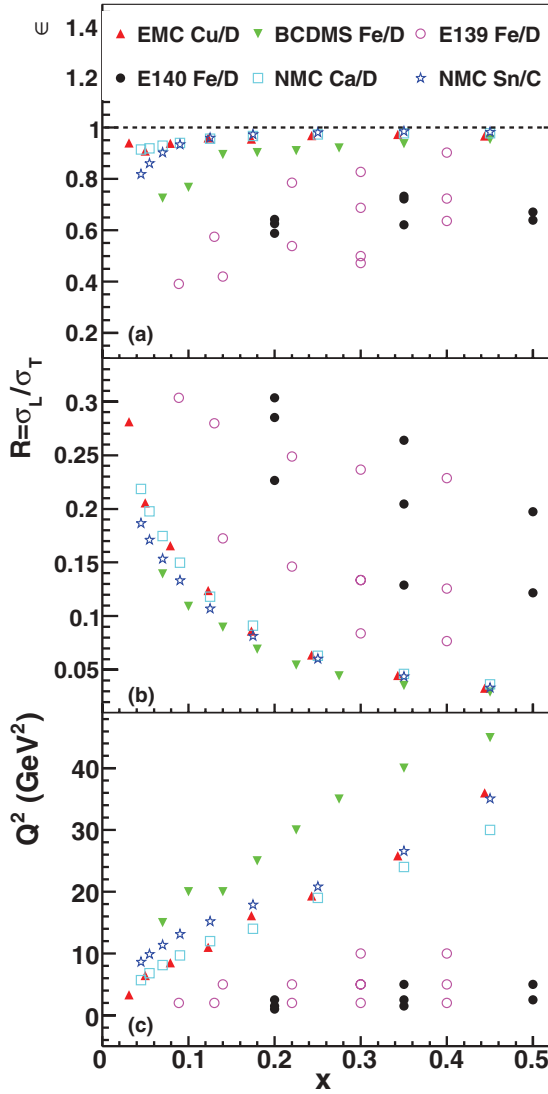


FIG. 2. (Color online) The kinematic coverage in Q^2 and x and the corresponding values of ϵ and R^N of the data points considered in this paper.

cross sections as

$$\begin{aligned} \frac{\sigma^A}{\sigma^D} &= \frac{F_2^A(x, Q^2)}{F_2^D(x, Q^2)} \frac{1 + R^D}{1 + R^A} \frac{1 + \epsilon R^A}{1 + \epsilon R^D} \\ &\approx \frac{F_2^A(x, Q^2)}{F_2^D(x, Q^2)} \left[1 - \frac{\Delta R(1 - \epsilon)}{(1 + R^D)(1 + \epsilon R^D)} \right], \end{aligned} \quad (6)$$

where the superscript A refers to the nucleus and the superscript D refers to the deuteron; $\Delta R \equiv R^A - R^D$. In the second line of Eq. (6) we used the expansion in terms of the small parameter ΔR and kept the first two terms of the expansion.

Alternatively, one can express the cross sections σ^A and σ^D in terms of the structure function $F_1(x, Q^2)$ and obtain

$$\begin{aligned} \frac{\sigma^A}{\sigma^D} &= \frac{F_1^A(x, Q^2)}{F_1^D(x, Q^2)} \frac{1 + \epsilon R^A}{1 + \epsilon R^D} \\ &= \frac{F_1^A(x, Q^2)}{F_1^D(x, Q^2)} \left[1 + \frac{\epsilon \Delta R}{1 + \epsilon R^D} \right]. \end{aligned} \quad (7)$$

The cross section ratio σ^A/σ^D can be identified with the structure function ratio F_2^A/F_2^D or F_1^A/F_1^D only with the assumption of the trivial nuclear dependence of $R = \sigma_L/\sigma_T$, i.e., $R^A = R^D$, or in certain kinematic limits. In particular, $\sigma^A/\sigma^D = F_2^A/F_2^D$ at $\epsilon = 1$ and $\sigma^A/\sigma^D = F_1^A/F_1^D$ at $\epsilon = 0$.

Figure 2 presents the kinematic coverage in Q^2 and x and the corresponding values of ϵ and R^N of the data points considered in this paper. On the one hand, the BCDMS [6], EMC [8], and NMC [10] data are mostly taken with ϵ close to unity [see Fig. 2(a)], which implies that the cross section ratios are close to the F_2 structure function ratios, even if $\Delta R \equiv R^A - R^D \neq 0$. On the other hand, the SLAC data [7,20] correspond to the kinematics where $\epsilon \approx 0.5$ [see Fig. 2(a)] and, hence, F_2^A/F_2^D will deviate from σ^A/σ^D if $\Delta R \neq 0$. For all these experiments $\epsilon \neq 0$ and, hence, the extraction of the transverse structure function ratios F_1^A/F_1^D depends explicitly on the assumption adopted for ΔR . Below we summarize what is known about it from the world data.

At small Q^2 , R might be different for deuterium and hydrogen [21], though it seems to be identical at large Q^2 [22,23]. In particular, there are some hints in both Thomas Jefferson National Accelerator Facility (JLab) E99-118 [21] and SLAC data [23] that R^D is smaller than R^H for $Q^2 < 1.5 \text{ GeV}^2$, with a global average of $R^D - R^H = -0.054 \pm 0.029$.

For heavier nuclei, the SLAC E140 data [20] suggest some nuclear dependence of R at $x = 0.2$, which seems to have a nontrivial Q^2 dependence ($R^{Fe} - R^D$ can be positive at $Q^2 = 2.5 \text{ GeV}^2$ and negative at $Q^2 = 1.5$ and 1 GeV^2):

$$\begin{aligned} R^{Fe} - R^D|_{Q^2=2.5} &= 0.144 \pm 0.079(\text{stat.}) \pm 0.027(\text{syst.}), \\ R^{Fe} - R^D|_{Q^2=1.5} &= -0.124 \pm 0.051(\text{stat.}) \pm 0.023(\text{syst.}), \\ R^{Fe} - R^D|_{Q^2=1} &= -0.086 \pm 0.057(\text{stat.}) \pm 0.022(\text{syst.}). \end{aligned}$$

A word of caution is in order here. Coulomb corrections may be non-negligible in DIS at SLAC and JLab kinematics, especially at large x . These corrections tend to reduce R for nuclear targets [24].

The nuclear dependence of R at Q^2 of the order of a few GeV^2 and lower was also measured by the HERMES Collaboration [11] by fitting the σ^A/σ^D cross section as a function of the virtual photon polarization ϵ over a typical range of $0.4 < \epsilon < 0.7$. Overall no significant nuclear dependence of R for ^{14}N and ^3He targets for $x > 0.06$ has been observed (the data in the $x < 0.06$ region are affected by the correlated background and should be neglected). However, since this was a single-energy measurement with correlated values of ϵ and Q^2 , the extraction of R^A/R^D was done in a model-dependent way.

At larger values of Q^2 , the NMC experiment [25] obtained $R^{Ca} - R^C = 0.027 \pm 0.026(\text{stat.}) \pm 0.020(\text{syst.})$ at $\langle Q^2 \rangle = 4 \text{ GeV}^2$ and concluded that ΔR is compatible with zero. However, a hint of the nontrivial nuclear dependence of R can be still seen in the data. The precision Sn/C data from NMC [26] show that $R^{Sn} - R^C = 0.040 \pm 0.021(\text{stat.}) \pm 0.026(\text{syst.})$ at a mean Q^2 of 10 GeV^2 . This value of $\Delta R \equiv R^A - R^D$ corresponds to $\Delta R/R^N = 0.22\text{--}1.20$, i.e., 22%–120% relative deviation for different values of x in the considered kinematics, where R^N is given by the parametrization of Ref. [18] presented in Fig. 2(b). Note that the extraction of ΔR in this experiment was based on a method closely related to

TABLE I. An overview of the measurements of the nuclear dependence of R discussed in this paper.

Experiment and observables	Kinematics	Beam energy
SLAC E140 [20] $R^{Fe,Au} - R^D$	$0.2 \leq x \leq 0.5$ $1 \leq Q^2 \leq 10 \text{ GeV}^2$	$3.7 \leq E \leq 15 \text{ GeV}$, up to five energies
NMC (1992) [25] $R^{Ca} - R^C$	$0.0085 \leq x \leq 0.15$ $1 \leq Q^2 \leq 15 \text{ GeV}^2$	$E = 90$ and 200 GeV , two energies
HERMES [11] $R^{3He,Ne}/R^D$	$0.01 < x < 0.8$ $0.2 < Q^2 < 3 \text{ GeV}^2$	$E = 27.5 \text{ GeV}$ single energy
NMC (1996) [26] $R^{Sn} - R^C$	$0.0125 \leq x \leq 0.45$ $3.3 \leq Q^2 \leq 35 \text{ GeV}^2$	$E = 120, 200, 280$ GeV , three energies

Rosenbluth separation that took advantage of three different incident muon energies (120, 200, and 280 GeV).

For convenience, we present in Table I a brief overview (covered kinematics in Bjorken x and Q^2 and energy settings) of the discussed measurements of the nuclear dependence of R (involving nuclei heavier than deuterium).

The results of the NMC measurement of $R^{Sn} - R^C$ as a function of Bjorken x [26] are presented as full squares in Fig. 3. For completeness, we also show the NMC result for the average $R^{Ca} - R^C$ [25] as an upward-pointing triangle, the SLAC E140 result for the average $R^{Au} - R^{Fe}$ [27] as a

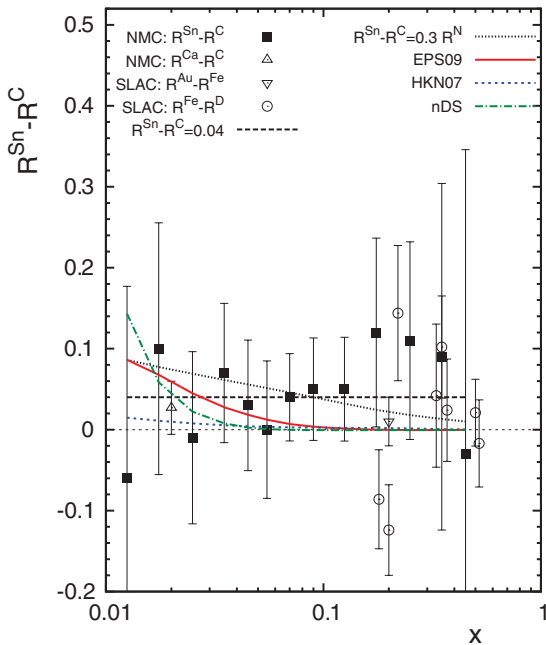


FIG. 3. (Color online) $R^{Sn} - R^C$ as a function of x . Full squares are results of the NMC measurement with the statistical and systematic errors added in quadrature [26]; the long-dash and dotted curves correspond to $R^{Sn} - R^C = 0.04$ and $R^{Sn} - R^C = 0.3R^N$, respectively; the curves labeled “EPS09,” “HKN07,” and “nDS” correspond to predictions using different nuclear parton distributions. Also shown are the NMC result for $R^{Ca} - R^C$ [25] (upward triangle), the SLAC result for $R^{Au} - R^{Fe}$ [27] (downward triangle), and SLAC E140 results for $R^{Fe} - R^D$ as a function of x [20] (open circles).

downward-pointing triangle, and the SLAC E140 results for $R^{Fe} - R^D$ as a function of x [20] as open circles. (For the latter, we showed only the data points for the 6% radiation length iron target and shifted them in x for better visibility.) The long-dash and dotted curves correspond to $R^{Sn} - R^C = 0.04$ and $R^{Sn} - R^C = 0.3R^N$, respectively. As one can see from the figure, both curves provide a good description of the measured values of $R^{Sn} - R^C$. Finally, the curves labeled “EPS09,” “HKN07,” and “nDS” correspond to the direct calculation of $R^{Sn} - R^C$ using different parametrizations of leading twist nuclear parton distribution functions (PDFs) (see the discussion in Sec. IV). Note that we have singled out the NMC Sn/C data [26] because the extraction of $R^A - R^D$ was done using a method closely related to the Rosenbluth separation and because the covered kinematics (the values of x , Q^2 , and ϵ) broadly overlaps with that of the BCDMS, EMC, and NMC data on σ^A/σ^D that we analyze in this paper.

In summary, as a global average, while R seems to show little nuclear dependence within relatively large experimental uncertainties, there exist hints of nontrivial nuclear dependence of R . In particular, $\Delta R = R^A - R^D$ may be statistically different from zero in some kinematics.

C. Impact of nuclear dependence of R on nucleus to deuteron structure function ratios

As we explained in Sec. II B, if there is a nontrivial nuclear dependence of R , the σ^A/σ^D cross section ratio is not equal to the F_1^A/F_1^D or F_2^A/F_2^D structure ratios. In particular, a positive $R^A - R^D$ will lead to $F_1^A/F_1^D < \sigma^A/\sigma^D < F_2^A/F_2^D$. Since the nuclear dependence of R has not as yet been systematically measured, we shall test two assumptions for ΔR that are motivated purely by the NMC Sn/C data [26], which has kinematic coverage similar to that of the BCDMS, EMC and NMC measurements. In our analysis below we assume the following:

- (1) (Absolute) $\Delta R = R^A - R^D = 0.04$. This is based on the NMC measurement of $R^{Sn} - R^C$ at an average $\langle Q^2 \rangle = 10 \text{ GeV}^2$.
- (2) (Relative) $(R^A - R^D)/R^N = 30\%$, which is possible in view of the fact that the NMC Sn/C data allow for the 22%–120% relative deviation of $\Delta R/R^N$.

Note that we effectively assumed that $R^A - R^D \approx R^{Sn} - R^C$, which corresponds to the lower limit for ΔR .

The impact of our assumptions for ΔR on selected nuclear DIS data is presented in Figs. 4 and 5. Note that we truncated the used data sets by neglecting low x and high x data points and focusing on the antishadowing region.

The BCDMS Fe/D [6], EMC Cu/D [8], and NMC Ca/D [10] data presented in Fig. 4 correspond to ϵ close to unity. Therefore, regardless of the assumption for ΔR , one expects that $F_2^A/F_2^D \approx \sigma^A/\sigma^D$ with a very good accuracy. On the other hand, F_1^A/F_1^D is clearly smaller than σ^A/σ^D . Thus, the few percent enhancement of σ^A/σ^D in the antishadowing region may be reduced or removed altogether for the ratio of the transverse structure functions F_1^A/F_1^D .

For the SLAC E139 [7] and E140 [20] Fe/D data presented in Fig. 5, the values of Q^2 are rather small [see Fig. 2(c)] and our assumptions for the nuclear dependence of R motivated

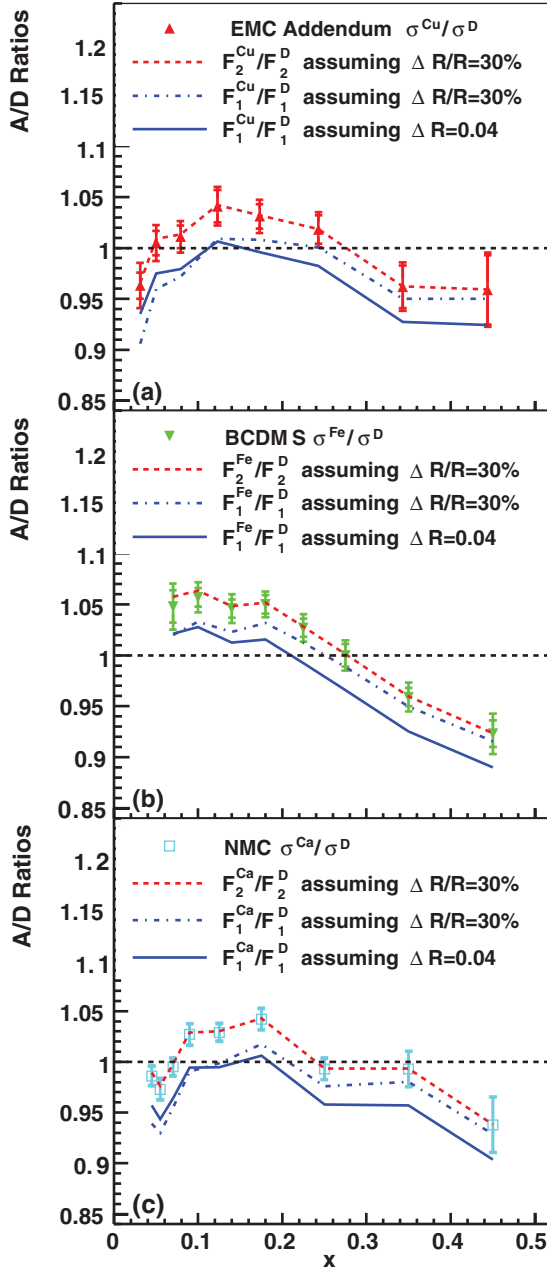


FIG. 4. (Color online) The impact of the nontrivial nuclear dependence of R on the structure function ratios around the antishadowing region for (a) EMC Cu/D [8], (b) BCDMS Fe/D [6], and (c) NMC Ca/D [10] data. The values of ϵ are close to unity.

by the NMC Sn/C measurement at higher Q^2 require a significant extrapolation in Q^2 . However, for the lack of better input, in our analysis of the SLAC data we adopt the same assumptions for ΔR as those used above. Since the values of ϵ for these two data sets are not close to unity [see Fig. 2(a)], $\Delta R > 0$ leads to noticeable differences between the ratio of the structure functions and the ratio of the cross sections according to the trend described by Eqs. (6) and (7): $F_1^A/F_1^D < \sigma^A/\sigma^D < F_2^A/F_2^D$.

In summary, the assumed nontrivial nuclear dependence of R leads to a decrease or to a complete disappearance (in

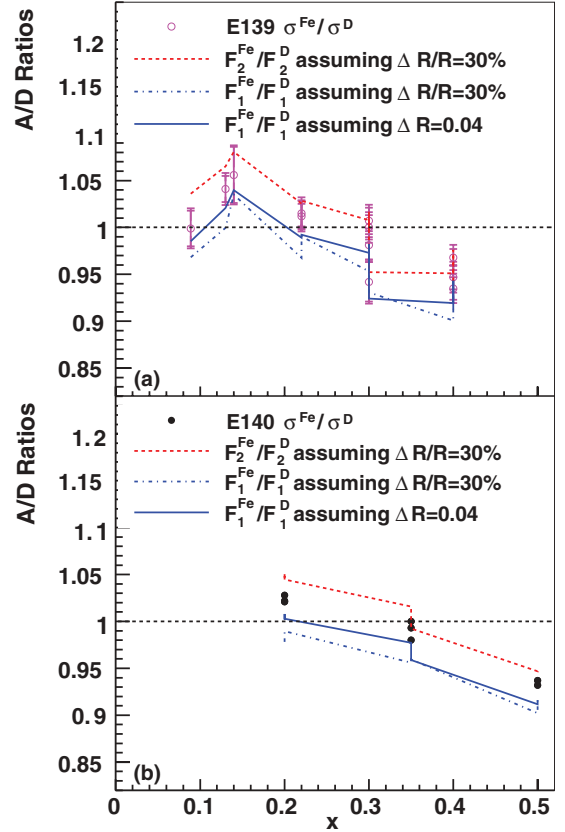


FIG. 5. (Color online) The impact of the nontrivial nuclear dependence of R on the structure function ratios around the antishadowing region for SLAC (a) E139 [7], and (b) E140 [20] Fe/D data.

some case) of enhancement of the F_1^A/F_1^D structure function ratio in the $0.1 < x < 0.3$ region. If confirmed by future experiments, this observation would indicate that the effect of antishadowing in σ^A is predominantly due to the contribution of the longitudinal structure function F_L^A , instead of F_1^A as implicitly assumed in most phenomenological analyses.

III. EXPERIMENTAL LIMITS ON DETERMINING $R^A - R^D$

Thus far we have examined the impact of a nuclear dependence of R on the extraction of the nuclear-dependent structure function ratios F_1^A/F_1^D and F_2^A/F_2^D from cross section ratios. The logical question then becomes “What is the limit on the experimental precision for $R^A - R^D$?” In this section we shall explore this question within the context of the precision likely to be available for the dedicated longitudinal/transverse (L/T) separation measurements over the next decade or two. For guidance we shall refer to the highest precision experiments performed at SLAC [7,20,23] and JLab [21,28]. These experiments have shown that reducing the σ^A/σ^D cross section ratio uncertainties, point to point in ϵ , below 1% is experimentally challenging, yet obtainable. For instance, the point-to-point uncertainties from JLab experiment E94110 [28] on cryogenic hydrogen have been estimated at about 1.5%, which was found to be consistent with the width of the distribution of residuals determined from the linear fits.

To measure cross sections at a range of ϵ values for fixed x and Q , both the SLAC and JLab inclusive L/T separation experiments utilized a range of beam energies in conjunction with well-studied spectrometer systems, which were able to be rotated to different angles and adjusted to accept varying ranges of momenta. Some of the largest contributions to the estimated systematic uncertainties stem from either time-dependent systematics, such as current calibrations or detector efficiency variations, or from the uncertainties in the kinematics at each beam energy and spectrometer setting. However, these systematics largely cancel in the cross section ratios, in which the electron yields on each target are taken at the same kinematic settings and close in time.

If, for example, a 3% antishadowing effect in F_2^A were entirely due to a longitudinal enhancement, with $F_1^A/F_1^D = 1$, then this would be reflected in a 3% slope in the cross section ratio versus $\epsilon' \equiv \epsilon/(1 + \epsilon R^D)$, corresponding to $\Delta R = R^A - R^D \approx 0.03$. For the current study we assume the following:

- (i) The total systematic point-to-point uncertainty (in ϵ) on the measured σ^A/σ^D ratios is 0.5%.
- (ii) There is no ϵ -dependent systematic uncertainty.
- (iii) There are six cross section ratio measurements at equally spaced $\epsilon' = \epsilon/(1 + \epsilon R^D)$ values in the range (0.05, 0.95), corresponding to six unique beam energies.

Under the assumptions above, we selected the cross section ratios at each ϵ' by random sampling from a Gaussian distribution assuming a 3% slope on σ^A/σ^D versus ϵ' and a Gaussian width of 0.5%. Six sample L/T separations generated by this procedure are shown in Fig. 6. After a linear fit was performed, the uncertainty on the measured slope was found to be 0.67%, corresponding to a 1σ (3σ) uncertainty on $R^A - R^D$ of less than 0.007 (0.021). For the case considered of 0.5% ratio uncertainties, one could determine at 1σ whether a 3% antishadowing effect is due mainly to F_L^A to $\approx 20\%$.

We note that this uncertainty on the extracted $R^A - R^D$ scales with the uncertainties on the cross section ratios such that a further reduction in the latter to 0.25% would reduce the

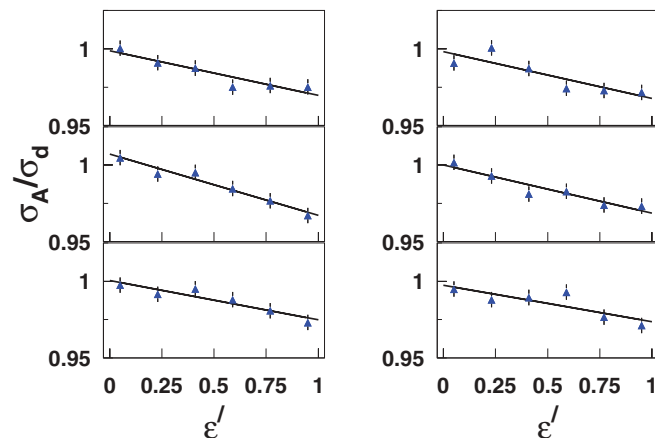


FIG. 6. (Color online) Random samples of the simulated σ^A/σ^D as a function of ϵ' (data points with error bars) and a linear fit (solid lines). (See the text for details.)

uncertainty on ΔR by half. However, we have thus far ignored any possible ϵ -dependent systematic uncertainties, such as those possibly arising from Coulomb and radiative corrections. For this reason, this is likely an optimistic scenario.

IV. NUCLEAR DEPENDENCE OF R AND ITS ROLE IN ANTISHADOWING OF THE GLUON DISTRIBUTION IN NUCLEI

We demonstrated in Sec. II C that the assumption of the nontrivial nuclear dependence of R , i.e., $R^A - R^D > 0$, whose magnitude and sign are motivated by the NMC Sn/C data [26], leads to a difference between the cross section and structure function ratios: $F_1^A/F_1^D < \sigma^A/\sigma^D < F_2^A/F_2^D$. Moreover, the reduction of the F_1^A/F_1^D ratio is quite sizable: the enhancement in the $0.1 < x < 0.3$ region visible in the cross section ratios is significantly decreased (or even disappears) for the F_1^A/F_1^D ratios, which indicates that antishadowing predominantly resides in the longitudinal structure function F_L^A . This conclusion is rather general; in particular, it does not rely on the twist expansion and the underlying partonic structure.

In the framework of the leading twist formalism, global QCD fits to the available data [13–17] show that the small enhancement of σ^A/σ^D in the antishadowing region translates into an enhancement of the valence quark and possibly gluon distributions in nuclei compared to those in the free proton. One should emphasize that in these analyses no nuclear dependence of R was assumed, i.e., $R = 0$. The pattern and magnitude of nuclear modifications of the nuclear gluon distribution $g_A(x)$ are known with very large uncertainty because $g_A(x)$ is mostly determined indirectly from scaling violations of the nuclear structure function F_2^A measured in a limited kinematics. This is illustrated in Fig. 7, where we present the ratio of leading-order gluon distributions in ^{40}Ca to that in the free proton, $g_A(x)/g_N(x)$, as a function of x at fixed $Q^2 = 3 \text{ GeV}^2$. In the figure, the solid curve is the result of the EPS09 fit [16]; the dotted curve is the result of the HKN07 fit [15]; and the dot-dashed curve is the nDS parametrization [14], whose results are quantitatively similar to those of [17]. For the EPS09 and HKN07 fits, we showed

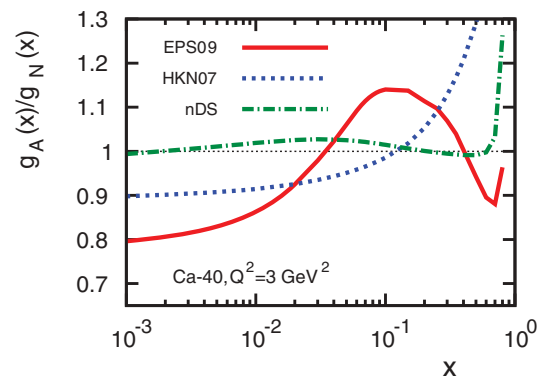


FIG. 7. (Color online) $g_A(x)/g_N(x)$ for ^{40}Ca as a function of x at fixed $Q^2 = 3 \text{ GeV}^2$ as obtained from global QCD fits. The solid, dotted, and dot-dashed curves are results of the EPS09 [16], HKN07 [15], and nDS [14] fits, respectively.

only the central values; the theoretical uncertainty on these predictions is quite large essentially in the entire range of x .

As one can see from Fig. 7, different groups predicts wildly different $g_A(x)/g_N(x)$ (with large uncertainties). Since the amounts of nuclear shadowing and antishadowing are correlated through the momentum sum rule, large antishadowing corresponds to significant shadowing in the EPS09 fit [16]; very small antishadowing corresponds to negligibly small shadowing in the nDS fit [14]); the HKN07 fit [15] suggests yet another scenario where large gluon antishadowing is concentrated at large x .

Given the present uncertainty in $g_A(x)$, it is important and instructive to confront the NMC measurement of $R^{Sn} - R^C$ [26] with direct calculations of this quantity in the framework of leading twist nuclear parton distributions. This is presented in Fig. 3, where the curves labeled “EPS09,” “HKN07,” and “nDS” correspond to the direct calculation of $R^{Sn} - R^C$ in the kinematics of the NMC measurement [26] using the respective leading-order parton distributions in nuclei. One can readily see from the figure that while for small x , $x < 0.05$, the leading twist description is consistent with our assumptions for $\Delta R \neq 0$ and the NMC data, in the antishadowing region $0.1 < x < 0.3$ and also for larger x the leading twist approach predicts a negligibly small ΔR in contrast with our assumptions and only marginally agrees with the data due to the large experimental uncertainty. Note that the leading twist calculations presented in Fig. 3 have rather small theoretical uncertainties stemming mostly from the uncertainty in the gluon distributions.

There are several reasons for the negligibly small value of $R^{Sn} - R^C$ for $x > 0.05$ at the NMC energies predicted in the leading twist framework. First and most importantly, the assumed shapes of the parametrizations of quark and gluon distribution in nuclei [14–17] are such that nuclear PDFs and the ratio R show only a weak nuclear dependence around $x = 0.1$ (see Figs. 7 and 8). For instance, while the EPS09 analysis [16] used the data on Q^2 dependence of $F_2^{Sn}(x, Q^2)/F_2^C(x, Q^2)$ [26], it did not include the $R^{Sn} - R^C$ data in the fit. Hence, the resulting nuclear PDFs were not constrained to reproduce the experimental values of $R^{Sn} - R^C$, which, as a result, leads to $R^{Sn} - R^C \approx 0$ for $x > 0.1$. Second, while R^{Sn}/R^N and R^C/R^N separately reveal quite sizable deviations from unity [compare to R^{Ca}/R^N presented in Fig. 8(a)], nuclear effects mostly cancel in the $R^{Sn} - R^C$ difference. In general, while it is natural to expect $\Delta R \neq 0$ because the pattern of nuclear modifications of quark and gluon distributions is different, with the currently assumed shapes of nuclear parton distributions it is not easy to generate sizable ΔR for $x > 0.1$ and large Q^2 because R itself is very small there. Third, in the NMC kinematics the values of Bjorken $x > 0.1$ correspond to $Q^2 > 10 \text{ GeV}^2$. At such large values of Q^2 , nuclear modifications of parton distributions gradually become less pronounced. Note also that it is unlikely that higher twist (twist-four) effects can generate sizable ΔR because it would require unrealistically large higher twist effects [2].

While the available data on the nuclear dependence of R are not able to constrain the nuclear gluon distribution in the $0.1 < x < 0.3$ region, a better chance of measuring gluon antishadowing would be offered by measurements of R with nuclear targets and the deuteron (proton) and at not too

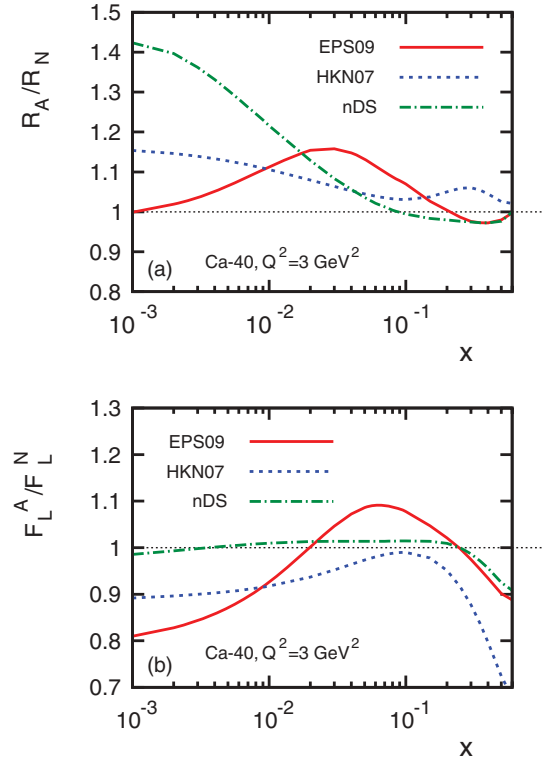


FIG. 8. (Color online) (a) R^A/R^N and (b) F_L^A/F_L^N for ^{40}Ca as functions of x at $Q^2 = 3 \text{ GeV}^2$. The solid, dotted, and dot-dashed curves are results of the EPS09 [16], HKN07 [15], and nDS [14] fits, respectively.

high Q^2 . Note that this is essentially equivalent to measuring the longitudinal structure functions $F_L(x, Q^2)$ for nuclei and the deuteron (proton). Such measurements can be carried out at JLab at 12 GeV at low-to-intermediate Q^2 [29] and at the future Electron-Ion Collider (EIC) at intermediate-to-high Q^2 [30,31]. In the latter case, the measurement of $F_2^A(x, Q^2)$ and the longitudinal nuclear structure function $F_L^A(x, Q^2)$ (by taking advantage of variable energies) with the subsequent extraction of $g_A(x)$ in a wide kinematic range is already an important part of the planned physics program.

An example of expected nuclear effects is presented in Fig. 8, which shows predictions for the ratio of the nuclear to nucleon ratios R^A/R^N (upper panel) and longitudinal structure functions F_L^A/F_L^N (lower panel) as a function of x at $Q^2 = 3 \text{ GeV}^2$ for ^{40}Ca . Different curves correspond to different parametrizations of nuclear PDFs (see Fig. 7). A comparison of Figs. 7 and 8 shows that different assumptions about the shape of the gluon (and quark) distributions in nuclei lead to different shapes of R^A/R^N and F_L^A/F_L^N . To point out just one feature, an observation of sizable $R^A/R^N > 1$ (enhanced F_L^A/F_L^N compared to F_1^A/F_1^N) and $F_L^A/F_L^N > 1$ in the antishadowing region $0.1 < x < 0.3$ would unambiguously signal the presence of a significant antishadowing for the gluon distribution in nuclei. (The gluon distribution enters the longitudinal structure function $F_L(x, Q^2)$ at the same order as the quark distributions; at the same time, the gluon distribution enters the transverse structure function $F_1(x, Q^2)$ with the weight (coefficient function) that is smaller

than that for $F_2(x, Q^2)$ [32].) The converse is also true: an absence of nuclear enhancement of R^A/R^N and F_L^A/F_L^N in the interval $0.1 < x < 0.3$ would translate into the absence of antishadowing for gluons in this region. It will be interesting to examine how these conclusions might effect the extraction of nuclear parton distributions from available and future data on nuclear structure functions using global QCD fits.

While in our work we focused of the antishadowing region, the nuclear dependence of R and its influence on the extraction of $F_2^A(x, Q^2)$ from the reduced cross section in the small- x (shadowing) region which can be probed at future lepton-ion colliders were examined in Ref. [33].

V. CONCLUSIONS

In this paper we studied the influence of the nontrivial nuclear dependence of $R = \sigma_L/\sigma_T$ on the extraction of the F_2^A/F_2^D and F_1^A/F_1^D structure function ratios from the data on the σ^A/σ^D cross section ratios. Guided by indications of the nuclear dependence of R from the world data and, in particular, by the NMC measurement that showed that $R^{Sn} - R^C = 0.040 \pm 0.021(\text{stat.}) \pm 0.026(\text{syst.})$ at $\langle Q^2 \rangle = 10 \text{ GeV}^2$ [26], we tested two assumptions for $\Delta R \equiv R^A - R^D$: $\Delta R = 0.04$ and $\Delta R/R^N = 0.3$, where R^N corresponds to the free proton [18]. With these assumptions, we examined selected sets of EMC, BCDMS, NMC, and SLAC data on σ^A/σ^D and extracted the F_2^A/F_2^D and F_1^A/F_1^D ratios. We found that for the EMC, BCDMS, and NMC data, $F_2^A/F_2^D \approx \sigma^A/\sigma^D$, while $F_1^A/F_1^D < \sigma^A/\sigma^D$. For the SLAC data, we found that $F_1^A/F_1^D < \sigma^A/\sigma^D < F_2^A/F_2^D$. In particular, we observed that the nuclear enhancement (antishadowing) in the interval $0.1 < x < 0.3$ becomes significantly reduced (or even disappears in some cases) for the ratio of the transverse structure functions F_1^A/F_1^D . The latter observation indicates that antishadowing may in fact be dominated by the longitudinal contribution rather than by the transverse one (i.e., antishadowing is dominated by gluons rather than by quarks) as implicitly assumed by current phenomenological analyses and global nuclear parton distribution fits. It will be interesting to examine

how our conclusion that antishadowing might be absent in the nuclear transverse structure functions affects extraction of nuclear parton distributions using global QCD fits.

We also examined experimental limits on determining $R^A - R^D$ from measurements of the $\epsilon' = \epsilon/(1 + \epsilon R^D)$ dependence of σ^A/σ^D . Making a plausible assumption that σ^A/σ^D has a 3% slope in ϵ' and can be measured with a 0.5% uncertainty over a broad range of ϵ' , we found that ΔR can be extracted with 0.67% uncertainty. Therefore, one could determine whether a 3% antishadowing effect is mainly due to F_L^A to approximately 20% accuracy.

In the leading twist framework, the magnitude of nuclear enhancement of R^A and the longitudinal structure function $F_L^A(x, Q^2)$ [quantities that directly probe the nuclear gluon distribution $g_A(x)$] is directly correlated with the size and shape of antishadowing for $g_A(x)$. While at the moment $g_A(x)$ is rather poorly constrained by QCD fits to available data, a dedicated high-precision measurement of the nuclear dependence of R [the longitudinal nuclear structure function $F_L^A(x, Q^2)$] at JLab and the EIC has the potential to unambiguously constrain $g_A(x)$ in the antishadowing region and beyond. [The EIC will also be able to constrain $g_A(x)$ deep in the shadowing region of small x .] Through the parton momentum sum rule, this knowledge will have a deep impact on $g_A(x)$ in the entire range of x . In particular, it should dramatically help to constrain $g_A(x)$ in the nuclear shadowing region, $10^{-5} \leq x < 0.05$, where $g_A(x)$ plays an essential role in phenomenology of high-energy hard processes with nuclei (for a review, see [34]).

ACKNOWLEDGMENTS

We are grateful to J. Gomez, W. Melnitchouk, P. Monaghan, and M. Strikman for helpful discussions. This work was supported by the US Department of Energy Contract No. DE-AC05-06OR23177, under which Jefferson Science Associates, LLC, operates Jefferson Lab, and US National Science Foundation Grant No. 1002644.

-
- [1] J. J. Aubert *et al.* (The European Muon Collaboration), *Phys. Lett. B* **123**, 275 (1983).
 [2] L. L. Frankfurt and M. I. Strikman, *Phys. Rep.* **160**, 235 (1988).
 [3] M. Arneodo, *Phys. Rep.* **240**, 301 (1994).
 [4] D. F. Geesaman, K. Saito, and A. W. Thomas, *Annu. Rev. Nucl. Part. Sci.* **45**, 337 (1995).
 [5] L. Frankfurt and M. Strikman, arXiv:1203.5278v1.
 [6] A. C. Benvenuti *et al.* (The BCDMS Collaboration), *Phys. Lett. B* **189**, 483 (1987).
 [7] J. Gomez *et al.*, *Phys. Rev. D* **49**, 4348 (1994).
 [8] J. Ashman *et al.* (The European Muon Collaboration), *Z. Phys. C* **57**, 211 (1993).
 [9] R. G. Arnold *et al.*, *Phys. Rev. Lett.* **52**, 727 (1984).
 [10] P. Amaudruz *et al.* (The New Muon Collaboration), *Nucl. Phys. B* **441**, 3 (1995).
 [11] K. Ackerstaff *et al.* (HERMES Collaboration), *Phys. Lett. B* **475**, 386 (2000); **567**, 339(E) (2003).
 [12] D. M. Alde *et al.*, *Phys. Rev. Lett.* **64**, 2479 (1990).
 [13] I. Schienbein, J. Y. Yu, C. Keppel, J. G. Morfin, F. Olness, and J. F. Owens, *Phys. Rev. D* **77**, 054013 (2008); I. Schienbein, J. Y. Yu, K. Kovarik, C. Keppel, J. G. Morfin, F. I. Olness, and J. F. Owens, *ibid.* **80**, 094004 (2009); K. Kovarik *et al.*, *Phys. Rev. Lett.* **106**, 122301 (2011).
 [14] D. de Florian and R. Sassot, *Phys. Rev. D* **69**, 074028 (2004).
 [15] M. Hirai, S. Kumano, and T. H. Nagai, *Phys. Rev. C* **76**, 065207 (2007).
 [16] K. J. Eskola, H. Paukkunen, and C. A. Salgado, *J. High Energy Phys.* **04** (2009) 065.
 [17] D. de Florian, R. Sassot, P. Zurita, and M. Stratmann, arXiv:1112.6324 [hep-ph].
 [18] L. W. Whitlow *et al.*, *Phys. Lett. B* **250**, 193 (1990); L. W. Whitlow, Ph.D. thesis, SLAC-Report-357, Stanford University, 1990.
 [19] K. Abe *et al.* (E143 Collaboration), *Phys. Lett. B* **452**, 194 (1999).

- [20] S. Dasu *et al.*, *Phys. Rev. D* **49**, 5641 (1994).
- [21] V. Tvaskis *et al.*, *Phys. Rev. Lett.* **98**, 142301 (2007); V. Tvaskis, Ph.D. thesis, Vrije Universiteit, Amsterdam, 2004.
- [22] M. Arneodo *et al.* (The New Muon Collaboration), *Nucl. Phys. B* **487**, 3 (1997).
- [23] L. H. Tao *et al.*, *Z. Phys. C* **70**, 387 (1996).
- [24] P. Solvignon, D. Gaskell, and J. Arrington, *AIP Conf. Proc.* **1160**, 155 (2009).
- [25] P. Amaudruz *et al.* (New Muon Collaboration), *Phys. Lett. B* **294**, 120 (1992).
- [26] M. Arneodo *et al.* (The New Muon Collaboration), *Nucl. Phys. B* **481**, 23 (1996).
- [27] S. Dasu *et al.*, *Phys. Rev. Lett.* **60**, 2591 (1988).
- [28] M. E. Christy *et al.* (E94110 Collaboration), *Phys. Rev. C* **70**, 015206 (2004).
- [29] L. Y. Zhu, M. E. Christy, C. E. Keppel, D. Gaskell, and P. Solvignon, JLab 12 GeV, proposal PR12-11-113 (2012) (unpublished).
- [30] D. Boer *et al.*, arXiv:1108.1713 [nucl-th].
- [31] A. Accardi, V. Guzey, A. Prokudin, and C. Weiss, *Eur. Phys. J. A* **48**, 92 (2012).
- [32] R. Brock *et al.* (CTEQ Collaboration), *Rev. Mod. Phys.* **67**, 157 (1995).
- [33] N. Armesto, H. Paukkunen, C. A. Salgado, and K. Tywoniuk, *Phys. Lett. B* **694**, 38 (2010).
- [34] L. Frankfurt, V. Guzey, and M. Strikman, *Phys. Rep.* **512**, 255 (2012).